THE ANNALS OF “DUNAREA DE JOS” UNIVERSITY OF GALATI.
FASCICLE IX. METALLURGY AND MATERIALS SCIENCE
N^0. 3 – 2012, ISSN 1453 – 083X

THERMAL DECOMPOSITION OF HAFNIUM ETHOXIDE-MOLLECULAR PRECURSOR FOR HAFNIA DIELECTRIC THIN FILMS

Elena Emanuela VALCU (HERBEI)[1], Viorica MUSAT[1], Timothy LEEDHAM[2]
[1]“Dunărea de Jos” University of Galaţi, Centre of Nanostructurs and Functional Materials, Romania,
[2] Multivalent Ltd. United Kingdoms
emails: viorica.musat@ugal.ro, tim.leedham@multivalent.co.uk

ABSTRACT

The HfO_2 thin-film is a very promising gate dielectric material for last generation transistors. The paper presents the thermal decomposition of hafnium ethoxide used as molecular precursor for obtaining hafnia thin films. The investigated molecular precursor is a mixture of $Hf_3O(OC_2H_5)_{10}$ and $Hf_4O(OC_2H_5)_{14}$ moisture sensitive amorphous powder.

The thermal decomposition of hafnium ethoxide precursor was investigated by TG-DTG-DSC analysis from room temperature to 600^0C in nitrogen atmosphere at 5K/min. The composition of gas products resulted during pyrolytic decomposition has been studied by Fourier Transformation Infrared Spectroscopy (FTIR) and Mass Spectroscopy (MS). In the gas products, hydrogen, methyl, ethyl, vinyl, hydroxyl groups, acetic aldehyde and acetylene were identified. From mass spectroscopy and FTIR data results that the loss of ethoxy groups from the molecular precursor occurs in the decomposition steps between 200 and 375°C. That suggests that in different steps, ligands from different coordination spheres are lost.

KEYWORDS: Hf-ethoxide, thermal behavior, dielectric thin films

1. Introduction

Hafnium dioxide (HfO_2) is a high temperature refractory material with very good dielectric properties [1]. The stoichiometric hafnium oxide has stable monoclinic structure. Heated at temperatures higher than 1700°C, it transforms into the tetragonal structure. Further heating at about 2700°C allows the further transformation into the cubic polymorphic form having the fluorite structure. A wide range of applications of HfO_2 such high-k gate electronic devices based on TFT [2- 5] as well as near-UV laser AR, dielectric mirror designs and waveguide [6] require thin film material. HfO_2 thin films and coatings can be prepared by various methods, as atomic layer deposition [8–11], pulsed laser deposition [12–14], chemical vapor deposition [15–17], radio frequency sputtering [18–20], plasma oxidation of Hf film [21] and sol–gel routes [22–34].

For MOCVD the preferred precursors are Hf t-butoxide and Hf ethylmethylamide for reasons of volatility. The great interest for using sol-gel method for preparation of films for multiple application fields is due to low fabrication costs with respect to other methods, advanced control of doping and the possibility of obtaining materials having a predetermined structure by modification of the elaboration parameters. The preparation of HfO_2 coatings by sol–gel method has been reported using different routes and precursors. Nishide *et al.* [22], Shimada *et al.* [23], Yu *et al.* [24], Shimizu *et al.* [25, 26] have prepared HfO_2 using $HfCl_4$ in ethanol as starting material. Takahashi and Nishide [27] and Nishide *et al.* [28] worked also with $HfCl_4$ but in water, hafnium hydroxide being an intermediate compound peptized with formic/oxalic acid. Blanc *et al.* [29] used the same Hf-source but in 1-methoxy 2-propanol. Aoki *et al.* [30] used $Hf(OBut)_4$ toluene/ethanol solution as a hafnium precursor. Goncalves *et al.* [31] used $HfOCl_2$ in ethanol as starting material. From the thermal decomposition of hafnium molecular precursors, nano size hafnium oxide or HfO_2-polymer hybrid thin films, can be obtained at low temperatures. The sol–gel preparation of HfO_2 thin films starting from Hf-ethoxide has been previously reported by several authors [6,33-34]. Villanueva-Ibanez *et al.* dissolved $Hf(OC_2H_5)_4$ in ethanol, in the presence of acetyl acetone [6]. Zaharescu *et al.* successfully prepared HfO_2 coatings on silicon wafer by sol–gel route from Hf-ethoxide, Hf-pentadionate and Hf-chloride precursors [34]. The films prepared from ethoxide and pentadionate precursors were homogenous and uniform with respect to their thickness before as well after crystallization. For this latter route, a nanoporosity was present in the quasiamorphous films as well in the crystallized ones. The molecular structure of Hf-oxo-ethoxide has been investigated by some authors [35], but the simple structure $Hf(OEt)_4$ has not been characterized.

In this paper we report the thermal behavior of hafnium ethoxide. A better understanding thermal behavior is very important to control the decomposition steps at different temperatures, and consequently the microstructure and properties of the obtained oxide films.

2. Experimental details

Hafnium ethoxide precursor was purchased from Multivalent Ltd. UK. The thermal analysis (about 10 mg samples weight) was carried out in dry nitrogen atmosphere using an Q5000 IR thermal analyses and a Q20 Differential Scanning Calorimeter, from Thermal Analysis Instruments, in a platinum crucible, at 5K/min rate up to 600°C. For the chemical composition of the gas products resulted during thermal decomposition of hafnium ethoxide, simultaneous thermogravimetric (TG-DTG), differential scanning calorimetry (DSC), Fourier transformation infrared spectroscopy (FTIR) and mass spectrometry (MS) analysis were conducted, using a NETZSCH simultaneous thermal analysis instrument coupled with FT-IR spectrometer QMS 403C and FTIR Spectrometer Vertex 70.

3. Results

Figure 1 shows the results of simultaneous TG-DTG-DSC data for precursor decomposition and the Gram Schmidt mass spectrometry curve of gas products resulting during this decomposition. The very complex decomposition process of hafnium ethoxide with mass change up to 375°C can be observed, with at least four important endothermic peak accompanied by release of gaseous products. The thermal decomposition begins with small mass loss processes (about 5% on TG curve) at ~ 85 and 155°C characterized by endothermic effects (DSC curve), accompanied by two small peak for released gaseous substances (curve Gram Schmidt). Extensive decomposition occurs between 160° and 340°C (with weight loss of ~70%) and intense endothermic DSC peaks at 280 and 356°C. From the DTG curve, one can observe that the most intense process is between 225° and 325°C, were the alkoxide losses the major weight percent (~60% of the hole mass loss).

The decomposition ends with an endothermic DSC peak at 356°C, accompanied by 10% of mass loss.

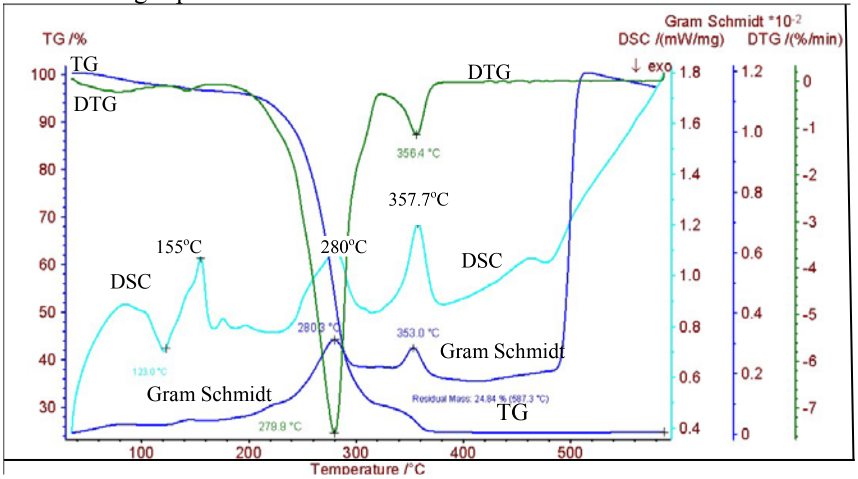

Fig. 1. *Experimental results of experimental curves recorded simultaneously during TG-DTG-DSC-MS analysis of hafnium ethoxide in dried nitrogen.*

Figure 2a reveals that the process with the highest mass loss and endothermic peak at 280°C is carried out with a much higher reaction rate (maximum rate of 7.5%/min) than the other decomposition steps. In the same time, Figure 2b shows that for this process (step 3) the thermal effect relative to the amount of substance decomposed is much lower than for the others steps. This means that the intermediate compound that decomposed at 280°C is less stable than the compound resulting from its decomposition and is less stable than the initial sample.

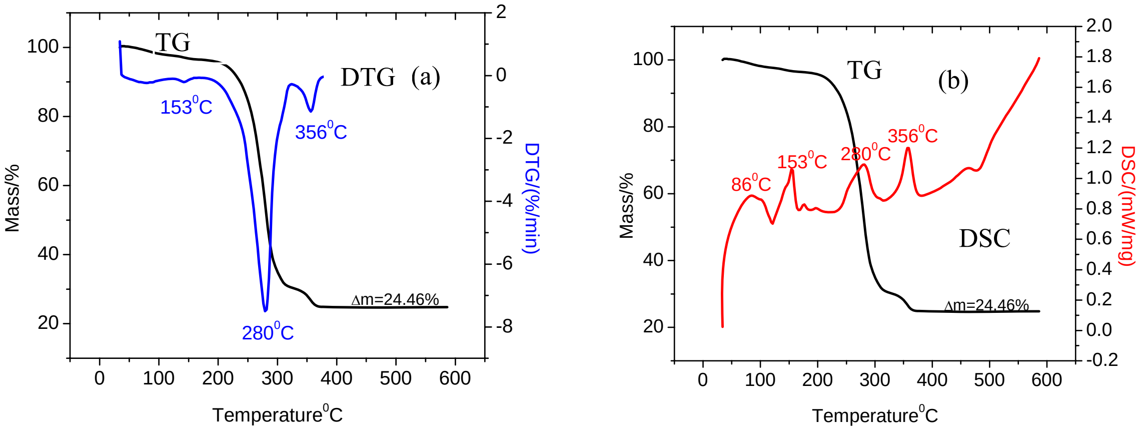

Fig. 2. *TG -DTG curves (a) and (TG-DSC) curves (b)*

In the range of room temperature (RT) to ~100°C, an evaporation process (2% weight loss) is observed. From 100° to 170°C other mass loss process (4% weight loss) occurs, very probably, the evaporation of some adducts existing in the sample of two alkoxides mixture. Between 170° to 375°C, the hafnia ethoxide clusters decompose with the formation of hafnium oxide and the release of different organics, as can be observed from the mass spectroscopy data (Fig. 3).

The gaseous products evolved during thermal decomposition were identified from mass spectroscopy (Fig. 3) and FTIR spectra (Fig. 4), such as: hydrogen, methyl, ethyl, vinyl, hydroxyl groups, acetic aldehyde and acetylene (Table 1).

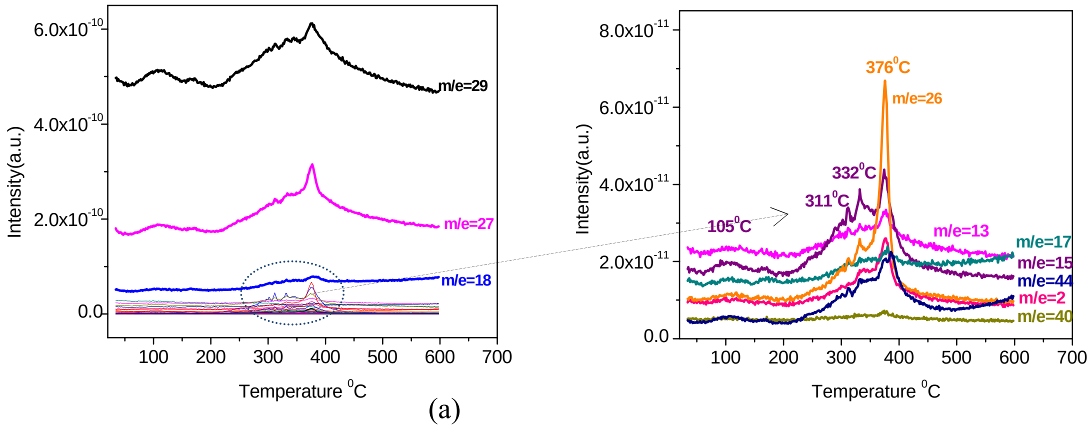

(a) (b)

Fig. 3. *Mass spectra of gas products of thermal decomposition of hafnium ethoxide, main peaks (a) and enlargement of smaller peaks (b).*

From FTIR spectra, one can conclude that, for the most important decomposition peaks (steps), the evolved gas correspond to the following chemical species: in the range of 893 – 950cm^{-1} the banding vibration of =C–H and =CH_2 (usually sharp) from the vinyl group, at 1750 cm^{-1} the stretching vibration for C=O from aldehyde, at 2973cm^{-1} and 1382cm^{-1} are the asymmetric vibrations of CH_3 in alkanes, at 1163cm^{-1} the vibrations of –CH_2 in alkanes, at 2315cm^{-1} is located the band of O=C=O and –H–C=O, and at 3250cm^{-1} are located the vibration of OH groups. The MS curves in Figure 3 confirm a decomposition process starting at 70^{0}C, in which the components are eliminated until 375^{0}C.

Taking into consideration the results previously discussed, the decomposition steps of the molecular precursor sample are:

- an evaporation process (4% weight loss), in the range of RT~100°C;
- the evaporation of some amount of adducts existing in the precursor sample, between 100-170°C;
- the main decomposition of cluster with the lost of majority of ethoxy groups and formation of other smaller clusters, between 200-320°C;

- the final decomposition of the clusters with the loss of last ethoxy groups and formation of hafnium oxide, between 320 - 375°C;
- the elimination of CH_3-CH_2 and CH_2=CH· radicals is demonstrated by both MS and FTIR spectra;
- for a better understanding of the decomposition mechanism of Hf-ethoxide molecular precursor, additional characterization of intermediaries products of the thermal decomposition steps mentioned before will be perform, using NMR and FTIR analysis methods.

Table 1. *TGA-DTG-DSC data of hafnium ethoxide decomposition*

ΔT (°C)	**T_{max} DSC peak (°C)**	**DSC peak**	**Weight loss (TG) (%)**	**Gas products (m/e values)**
35-123 123-170	86 153	Endo Endo	4 2	H_20 (m/e=18) 2 CH_3-CH_2- (m/e=29) 2 CH_2=CH- (m/e=27)
200-320 320-375	280 356	Endo Endo	60 10	CH_3-CHO (m/e=44) CO_2 (m/e=44) CH_3-CH_2- (m/e=29) CH_2=CH- (m/e=27) C_2H_2- (m/e=26) OH- (m/e=17) CH_3- (m/e=15) CH- (m/e=13) H_2 (m/e=2)

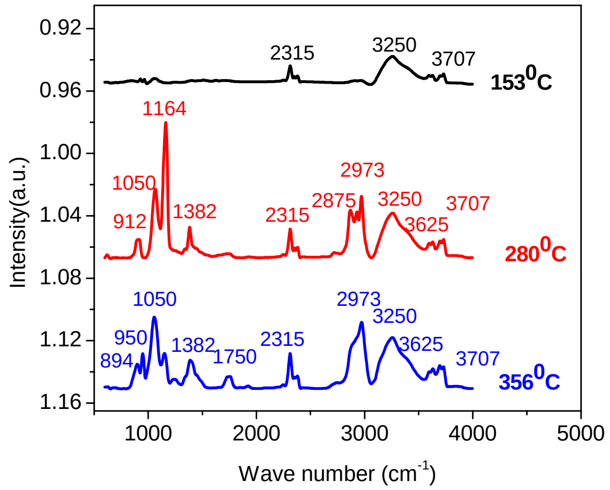

Fig. 4. *FTIR absorption spectra of gas products resulted from thermal decomposition of hafnium ethoxide*

Conclusions

The thermal decomposition of hafnium ethoxide precursor was investigated by TG-DTG-DSC analysis from room temperature to 600^{0}C in nitrogen atmosphere, coupled with Fourier transformation infrared spectroscopy and mass spectrometry analysis of gas products.

Hafnium ethoxide molecular precursor decompose in four steps below 356^{0}C, and can be used for sol-gel synthesis of HfO_2 polycrystalline thin films or hybride nanocomposite thin films. From mass spectroscopy and FTIR data results that the loss of ethoxy groups from the molecular precursor occurs in the decomposition steps between 200 and 375^{o}C. That suggests that in different steps, ligands from different coordination spheres are lost.

Acknowledgements

This work was supported by projects FP7-POINTS No. 263042 and 156EU-POINTS.

The work of Elena-Emanuela Valcu was supported by Project SOP HRD – TOP ACADEMIC 78622.

References

[1]. Wang J, Li HP, Stevens RJ - Mat Sci 27:5397, (1992).

[2]. Haussa M, Pantisano L, Ragnarsson LA, Degrave R, Schram T, Purtois G, De Gendt S, Grosenken G, Heyns MM - Mat Sci Eng R51:37, (2006).

[3]. Bersuker G, Zeitzoff P, Brown G, Huff HR - Mater Today 7(1):26, (2004).

[4]. Brezesinski T, Smarsly B, Iimura K, Grosso D, Boissiere C, Amenitsch H, Antoinietti M, Sanchez C - Small 1:889, (2005).

[5]. Supplit R, Husing N, Gross S, Bernstoff S, Puchberger M - Eur J Inorg Chem 18:2797, (2007).

[6]. Villanueva-Ibanez M, Le Luyer C, Marty O, Mugnier J - Opt Mater 24(1–2):51, (2003).

[7]. Villanueva-Ibanez M, Le Luyer C, Parola S, Marty O, Mugnier J - Rev Adv Mater Sci 5:296, (2003).

[8]. Boher P, Defraneaux C, Heinrich P, Wolsenholme J, Bender H - Mat Sci Eng B109:64, (2004).

[9]. Ferrari S, Modreanu M, Scarel G, Fancinelli M - Thin Solid Films 450:124, (2004).

[10]. Hausmann DM, Gordon RG - J Cryst Growth 249:251, (2003).

[11]. Kim YW, Roh Y, Yoo JB, Kim H - Thin Solid Films 515:2984, (2007).

[12]. Essary C, Howard JM, Craciun V, Craciun D, Singh RK - Thin Solid Films 450:111, (2004).

[13]. Wang SJ, Lim PC, Huan ACH, Liu CL, Chai JW, Chow SY, Pan JS, Li Q, Ong K - App Phys Lett 82–13:2047, (2003).

[14]. Lee PF, Dai JY, Chen HLW, Choy CL - Ceram Int 30:1267, (2004).

[15]. Fang Q, Zhang JY, Wang Z, Modreanu M, O’Sullivan BJ, Hurley PK, Leedham TL, Huywel D, Audier MA, Jiminez C, Senateur JP, Boyd JW - Thin Solid Films 453–454:203, (2004).

[16]. Fang Q, Zhang JY, Wang ZM, He G, Yu J, Boyd JW - Microel Eng 66:621, (2003).

[17]. He JQ, Teren A, Jia CL, Ehrhart P, Urban K, Waser R, Wang RH - J Cryst Growth 262:295, (2004).
[18]. Pereira L, Maques A, Aguas H, Nevedev N, Georgiev D, Fortunato E, Martinis R - Mat Sci Eng B109:8917, (2004).
[19]. Lee BH, Kang L, Nieh R, Qi WJ, Lee JC - App Phys Lett 76–14:1926, (2000).
[20]. Gruger H, Kunath Ch, Kurth E, Sorge S, Pufe W, Pechstein T. - Thin Solid Films 447–448:509, (2004).
[21]. He G, Fang Q, Liu M, Zhu LO, Zhang LD - J Cryst Growth 268:155, (2004).
[22]. Nishide T, Honda S, Matsuura M, Ide M - Thin Solid Films 37:61, (2000).
[23]. Shimada S, Sato T - Carbon 40:2469, (2002).
[24]. Yu JJ, Fang Q, Zhang JY, Wang ZM, Boyd IW - App Surf Sci 208–209:676, (2003).
[25]. Shimizu H, Asayama K, Kawai N, Nishide T - Japan J Appl Phys 43:6992, (2004).
[26]. Shimizu H, Sato T, Konagai S, Ikeda M, Takahashi T, Nishide T. - Jpn J Appl Phys 46:4209, (2007).
[27]. Takahashi T, Nishide T - J Ceram Soc Jpn Suppl 112-1 PacRim5 Special Issue 112(5):S234–S238, (2004).
[28]. Nishide T, Meguro T, Suzuki S, Yabe T, - J Ceram Soc Jpn 113:77, (2005).
[29]. Blanc P, Hovnanian N, Cot D, Larbot A - J Sol-Gel Sci Technol 17:99, (2000).
[30]. Aoki Y, Kunitake T, Nakao A - Chem Mater 17:450, (2005).
[31]. Goncalves RR, Carturan G, Zampedri L, Ferrari M, Montagna M, Chiasera A, Righini GC, Pelli S, Ribeiro SLJ, Messaddaq Y - Appl Phys Lett 81–1:28, (2002).
[32]. Phani AR, Passacantando M, Santucci S - J Non-Cryst Solids 353:663, (2007).
[33]. Tardy J, Erouel M, Deman AL, Gagnaire A, Teodorescu V, Blanchin MG, Canut B, Barau A, Zaharescu M. - Microel Reliab 47:372, (2007).
[34]. Zaharescu M, Teodorescu VS, Gartner M, Blanchin MG, Barau A, Anastasescu M. - J Non-Cryst Solids 354:409, (2008).
[35]. Mayer M - SIMNRA Users Guide, Report IPP 9/113, Max, (1997).
[36]. Sergej Paskoa, Liliane G. Hubert-Pfalzgraf, Adulfas Abrutisb, T - Materials Letters 59, 1836– 1840, (2005).